Effects of inert gas jet on the transition from deflagration to detonation in a stoichiometric methane-oxygen mixture

Jun Cheng[1], Bo Zhang[1†], Hoi Dick Ng[2], Hong Liu[1], Fuxing Wang[1]

[1]Shanghai Jiao Tong University
School of Aeronautics and Astronautics, Shanghai, 200240, China

[2] Concordia University
Department of Mechanical, Industrial and Aerospace Engineering
Montréal, QC, H3G 1M8, Canada

[†]Corresponding Author

E-mail: bozhang@sjtu.edu.cn

Abstract

Detonation is an energetic combustion mode augmenting high flow momentum and thermodynamic efficiency, it has been applied in detonation engines, such as pulse detonation engines (PDEs) and rotating detonation engines (RDEs), they have become potential aerospace propulsion equipment. Recently, fluidic jet-in-cross flow (JICF) has been demonstrated experimentally and numerically that can accelerate the deflagration-to-detonation transition (DDT) process. Nonetheless, most of previous studies focused on the jets using combustible mixture or oxygen, which may bring additional risk for turbulence-generated system in detonation engines. In this study, a more safe and controllable inert gas (i.e., Ar) is applied for JICF, experiments are carried out to investigate effects of argon jet as an enhancement method on promoting the DDT in a stoichiometric methane-oxygen mixture. The effects of local argon concentration, turbulence intensity and injection position on the DDT process are systematically examined. Two-dimensional numerical simulations are also performed to elucidate the details of the injection evolution. The experimental results show that turbulence generated by the argon injection can promote flame acceleration and the onset of detonation only in the fast deflagration regime. The enhancing effect is more prominent at higher turbulence intensity by increasing jet injection pressure and shorter injection time. Too long injection duration increases argon local concentration that leads to an adverse effect prohibiting the DDT occurrence. During the initial laminar flame acceleration, referred to as the slow deflagration regime, no enhancement by the argon jet on DDT can be observed. By looking numerically at the flow structure of the argon jet, the vortical features enhance the transport and mixing between reactants and products. The interaction between the reactive travelling wave and the jet structure further induces turbulence and thus accelerates the chemical reaction rate. With the time elapsed, the injected argon entrains largely and dilutes the ambient combustible mixture, and restrains the

DDT. Furthermore, a novel dimensionless criterion and a characteristic parameter Tur_c are proposed, quantitatively analyzing the dominate mechanism in flame propagation and the initial stage of DDT as inert jet is introduced.

Keywords: Jet flow; Inert gas; Turbulence; Detonation; DDT

1. Introduction

In recent years, there is an increasing interest in developing detonation-based engines, such as Pulsed or Rotating Detonation Engines (PDEs or RDEs) for hypersonic propulsion applications [1-3]. One of the major challenges in designing these propulsive systems is the capability to initiate a detonation in a chamber of limited size [4-6], wherein the detonation propagation limits are a key as well as the fundamental problem for maintaining the propagation of detonations without failure to sustain their propulsion trust [7-9], this topic has been widely investigated as the detonations propagate though obstacles in recent years by Zhang et al. [10-12] , Cao et al. [13] and Gao et al. [14-16].

A detonation can be initiated by direct or indirect ways [17-19]. Direct initiation refers to an instantaneous detonation formation using a large energy deposition into the explosion [20, 21]. Such initiation method is impractical for engineering applications in most industrial settings. Alternatively, a detonation can be formed by indirect way, referring to the deflagration-to-detonation transition (DDT) [22, 23]. It requires a weak ignition source and DDT is achieved after different stages of flame acceleration from slow burning to high speed turbulent deflagration, and eventually the detonation onset for various physical mechanisms involved [24-26]. In smooth tubes, the distance from the ignition to the onset of detonation, named as the DDT run-up distance, can be very long. A wealth of experimental and numerical studies thus focus on finding most effective flame acceleration configurations to achieve DDT in short run-up distance. Since the pioneer work of Shchelkin [27], turbulence is known to play a significant role on the flame acceleration. Hence, over the past decades, the use of repeated obstacles to generate turbulence in the path of flame propagation to promote DDT has been extensively researched [28-30].

Although physical obstacles can prominently promote DDT, but they also induce significant pressures losses in the process. Cooper *et al.* [31] pointed out that the obstacles can reduce the impulse of a single-cycle PDE by up to 25%. Recently, Knox *et al.* [32] introduced a fluidic jet obstacle as an alternative to conventional DDT enhancement devices for turbulence generation. They compared the relative performance of fluidic and physical obstacles on DDT, and found that both the intense turbulent mixing characteristics inherent of a high-velocity jet and the blockage created by the virtual obstacle can significantly facilitate flame acceleration and transition to detonation.

To systematically investigate turbulence-induced DDT, Chambers & Ahmed [33] focused experimentally on the flame acceleration regime in a highly turbulent environment. They looked at experimentally and classified characteristics of turbulent flame dynamics and fast flame propagation modes at various regimes. The critical stage for turbulence driven deflagration to detonation of fast flames was closely examined. McGarry & Ahmed [34, 35] and later Chambers & Ahmed [36] and Tarrant *et al.* [37] examined interaction mechanisms of the propagating flame with turbulence induced by a fluidic jet, specifically analyzing the resulting flame-turbulence interaction modes and their influence on the flame propagation dynamics. Recently, Peng *et al.* [38] investigated the effects of fluidic jet-in-crossflow (JICF) on flame acceleration and DDT. They used a reactive transverse CH_4-O_2 mixture as jet in crossflow, showing promising enhancement on flame acceleration.

JICF has been proven promising as a practical, efficient method to accelerate flame propagation and promote DDT with less overall pressure losses [39-41]. It is noteworthy that most JICF enhancers used combustible gases. Such use may bring more uncontrollable factors and increase the risk for the turbulence-generated system in detonation-based propulsion devices. Up-to-date, studies using inert gas for JICF and investigating its effect on flame acceleration and

DDT behavior are scarce. Hence, in this work, the effects of inert argon jet with different injection conditions on DDT are explored via experiments and numerical simulations. Piezoelectric probes are used to measure the time-of-arrival of the leading travelling wave and such velocity results are then used to characterize different flame propagation regimes. The unsteady argon jet structures are analyzed using two-dimensional numerical simulations. The present results can thus advance understanding of the influencing mechanism of the inert gas JICF on flame acceleration and DDT.

2. Experimental Details and Numerical Methodology

2.1 Experiments

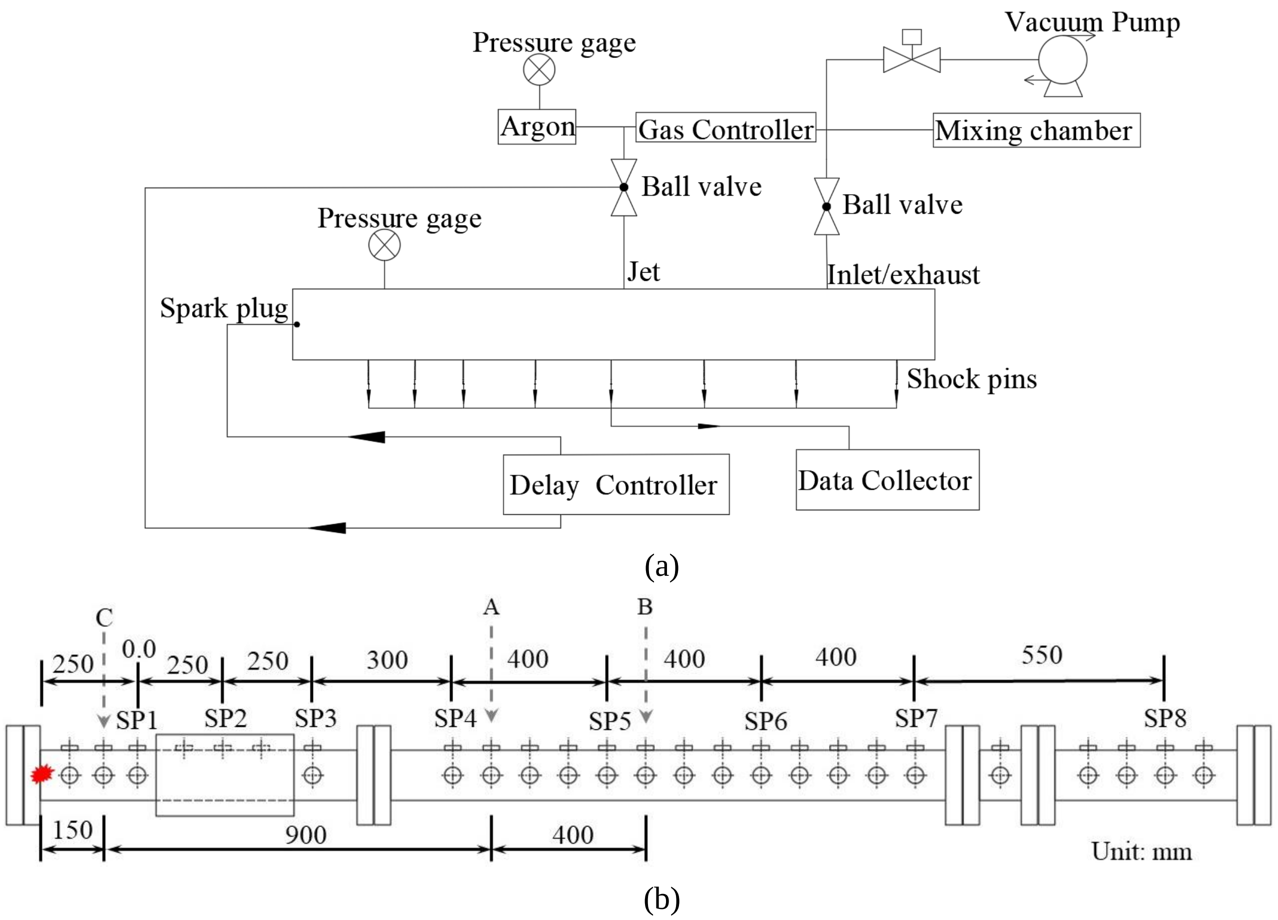

Fig. 1 Sketch of the experimental setup. a) A schematic of the experiment system; and b) shock pins and jet positions (A, B and C).

Figure 1a shows a schematic of the experimental facility which consisted of the fuel/oxygen mixing system, argon gas supply, ignition system, delay control system, data acquisition, gas controller and the shock tube, more details can be found in authors' previous literature [42, 43]. The methane fuel and oxygen was homogeneously mixed at the stoichiometric ratio for 24 h in a 180-L mixing chamber. The spark plug was placed at the center of the left end wall. The delay control system is composed of ARM-STM32F103CB development boards and an Ingenex-H3MB-052D solid-state relay; the arrows from the delay controller in Fig. 1a denote the signals sent to the ignition spark and the solenoid valve.

The stainless steel tube has a length of 2950-mm long and a 100 mm×100 mm cross-section. It was divided into four parts connected by flanges. Eight Dynasen shock pins (CA-1134) were used to capture the time-of-arrival (TOA) of the leading shock wave, and the shock pins arrangement is shown as SP1 to SP8 in Fig. 1b. The argon supply system includes a solenoid valve (AM230C), a one-way valve and a 2.4-L tank. The solenoid valve response time is 7 ms. Three jet positions (A, B, C) were chosen to investigate the effect of jet location on DDT. The distance relative to the position of SP1 was 0.9, 1.3 and -0.1 m for A, B and C jet position, respectively. The mixture was ignited by a 40-J spark. The mixture initial pressure was monitored by OMEGA digital gauges (PXM00710V, 0-700 kPa with an accuracy of ±0.25% full scale).

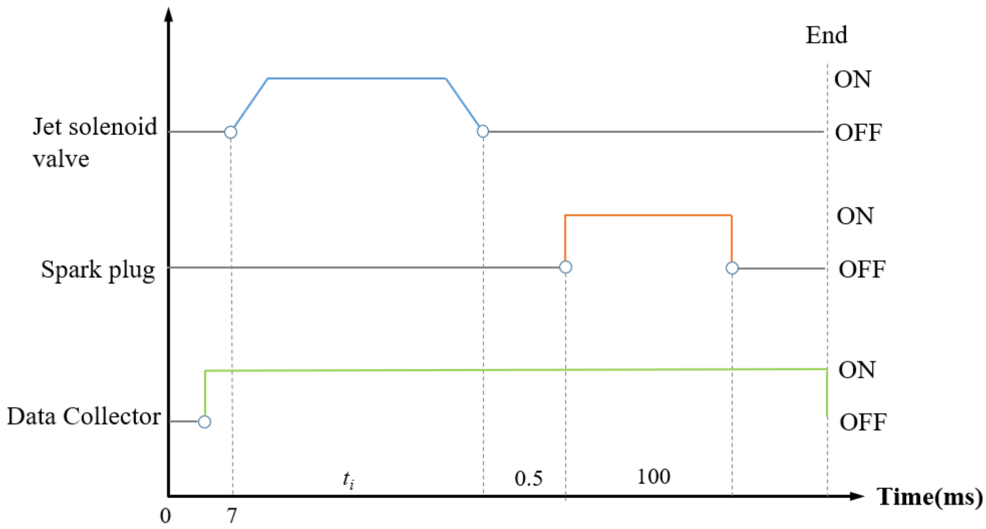

Fig. 2 Time sequence of the control signals.

Before each experiment, the tube was evacuated to about 0.1 kPa (absolute pressure), and then filled with the combustible mixture from the mixing chamber, controlled by the gas controller to a desired initial pressure, P_0. The 2.4-L storage bottle was filled with argon at a high initial injection pressure, P_i. Figure 2 shows the time sequence of the signals sent to the solenoid valve and the spark igniter. The argon injection was triggered first by opening the solenoid valve for a duration t_i. The igniter was then fired after 0.5 ms. The whole process was recorded by the data acquisition system.

In this study, the initial mixture pressure P_0 was kept at 25 kPa and the initial temperature 300 K. Various injection pressures and durations were used to investigate the influence of the generated turbulence characteristics and local argon concentration on DDT. Four groups of experiments were designed to examine effects of each individual factor.

2.2 Numerical simulations

As the turbulence structure induced by the jet had fully developed before the ignition was triggered, therefore a series of large eddy simulations were carried to investigate the turbulence characteristic under different injection conditions. The process of Ar injected into the tube was simulated by two dimensional (2D) Navier-Stokes equations. A Roe Riemann solver was utilized to construct numerical upwind fluxes, and the Minmod limiter with MUSCL reconstruction was applied to construct a third-order method in space. The time integration was advanced using a fourth-order explicit Runge–Kutta algorithm. Two different injection positions were chosen to compare the turbulence structure evolution while Ar was being injected into the tube, two schematics are shown in Fig. 3. To improve the efficiency of calculation, the length of the domain was reduced to 1.5 m and 0.8 m respectively for diagram (a) and (b). The left and right boundary conditions were set as pressure far-field, the upper and bottom sides were set as adiabatic walls. The jet velocity was given by an average value (approximately 100 m/s) in the process of injection, based on the calculation of injection pressure (P_j) was 200 kPa. The initial pressure P_0 was 25 kPa and the temperature T_0 was 300 K. In order to keep consistent with the experimental conditions, the jet was shut down for 0.5 ms when the injection time t_i was 15 ms, 25 ms, 50 ms, 75 ms and 100 ms. The mesh was set adaptively refined with the gradient of the concentration of Ar. The base size of the mesh was 0.5 mm, and the minimum mesh was refined to 0.0625 mm.

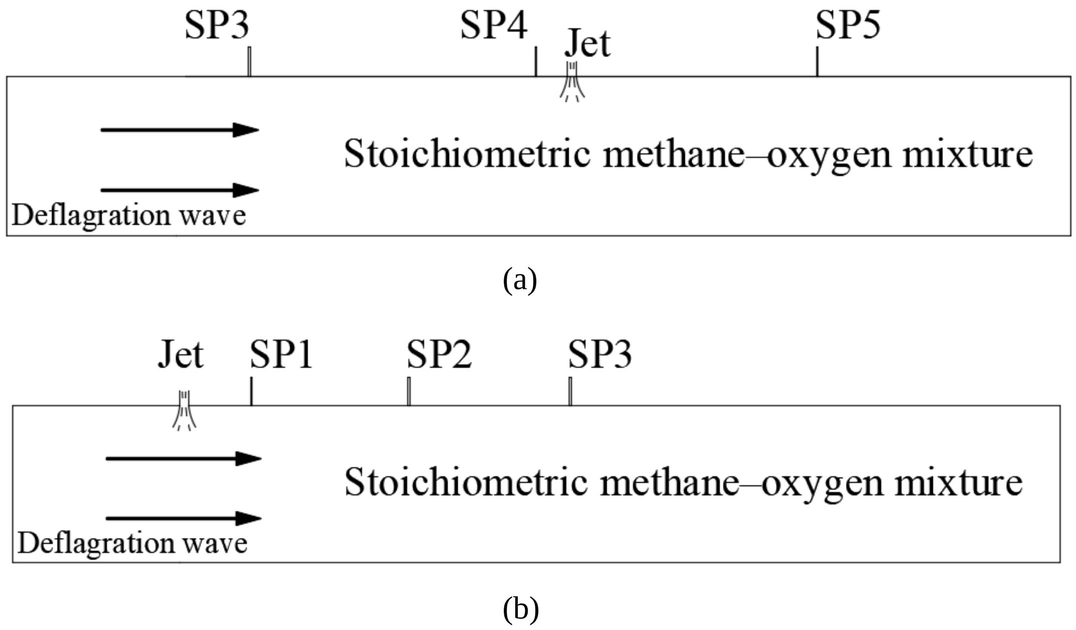

Fig. 3 A schematic of the simulation setup with different jet positions.

3. Results and Discussion

3.1 The effect of jet injection pressure

To distinguish the impact of P_i on DDT, four experimental cases are designed (Table 1). Case A0 represents the flame propagation in the tube without argon jet and used as the baseline case. Cases A1 to A3 consider different injection pressure but at a fixed injection duration and position.

Table 1 Injection parameters for experiments with varying injection pressure.

Case #	P_i/kPa	t_i/ms	Position
A0	0	0	N/A
A1	100	15	A
A2	150	15	A
A3	200	15	A

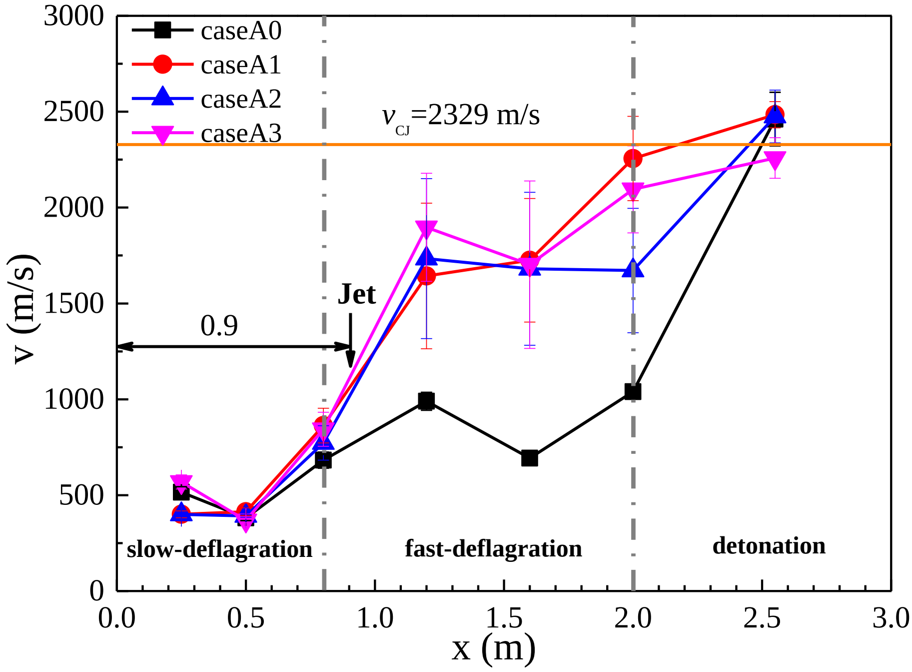

Fig. 4 Velocity of the lead wave with different argon injection pressure P_i.

Figure 4 shows the leading wave velocity behavior for the cases without (case A0) and with argon injection (cases A1 to A3). The data points correspond the shock pins location, starting with SP2 as the first point. The *y*-axis is the average velocity calculated between the adjacent shock pins. From the baseline case A0 velocity results, one can deduce correspondingly the wave propagation dynamics into three stages. The first is related to the slow deflagration burning from the ignition point to the location of SP4 (x = 0.8 m), and the wave velocity remains approximately 500 m/s. When the flame accelerates, the leading shock strengthens to almost a velocity about 1000 m/s. This second stage is referred to as the fast deflagration in this study, from SP4 to SP7 (x = 2.0 m) along the tube. Subsequently, DDT occurs near the end of the tube from SP7 to the SP8 (x = 2.55 m). In this last stage, the wave propagation velocity reaches the theoretical C-J detonation velocity. Therefore, under the condition of quiescent state (case A0), a slow deflagration is first ignited by the spark, and then a turbulent deflagration accelerates to half the CJ velocity (~1000 m/s), which is the typical condition observed in DDT prior to the onset of detonation [4].

For cases A1 to A3, a vertical argon jet is introduced at a location near SP4 prior to the arrival of the reactive wave complex and the results are also given in Fig. 4. The velocity behavior shows noticeably a significant difference compared with the baseline case A0. The argon jet leads to an abrupt wave acceleration. The results show that, although P_i is different for each case, all starts to accelerate abruptly from x = 0.8 m to an average velocity about 1860 m/s and an earlier DDT. The error bars shown on the plot represent the variations between repeated shots (more than 5) with the same initial condition. With the argon jet, the flow field experiences different levels of turbulence perturbation, causing a larger velocity variation between shots in the fast deflagration regime perturbed by the argon jet.

When the injection forms certain turbulent structure in the tube, it changes the local combustible mixture concentration near the jet. Therefore, it is necessary to define how dynamically the injection accelerates the wave propagation. From the fluid dynamic point-of-view, the turbulence effect can be divided into two simple physics problems [44]. One is the flame interaction with the vortex introduced by the injection due to the Kelvin-Helmholtz (K-H) instability, the other is the Richtmyer–Meshkov (R-M) instability when the lead shock passed through the mixture with density gradient. Both turbulence generation mechanisms may contribute to the wave acceleration. It is noteworthy that as an inert gas, the injected argon can have a negative effect on the combustion process due to the dilution and reduce the reactivity of the mixture and hence, slow down the flame propagation. Nonetheless, Fig. 4 demonstrates that under the specific conditions given in Table 1, the turbulence mechanism dominates, providing a positive effect on the flame acceleration. However, a competitive effect exists between the level of argon concentration and turbulence generation effect by the argon jet.

3.2 The effect of local argon concentration

The second set of experiments were performed to look at the argon concentration effect on the wave acceleration and DDT. Experiments with a fixed P_i but variable t_i at location A were considered (Table 2). The case B0 is the baseline without any argon injection. Note that the local argon concentration in the tube increases as t_i increases. However, as P_i is kept constant, the injection velocity is almost the same for the cases B1 to B6, which ensures the turbulence effect due to jet injection remains at the same level.

Table 2 Injection parameters for experiments with varying local argon concentration.

Case #	P_i/kPa	t_i/ms	Position
B0	0	0	N/A
B1	200	15	A
B2	200	25	A
B3	200	50	A
B4	200	100	A
B5	200	200	A
B6	200	400	A

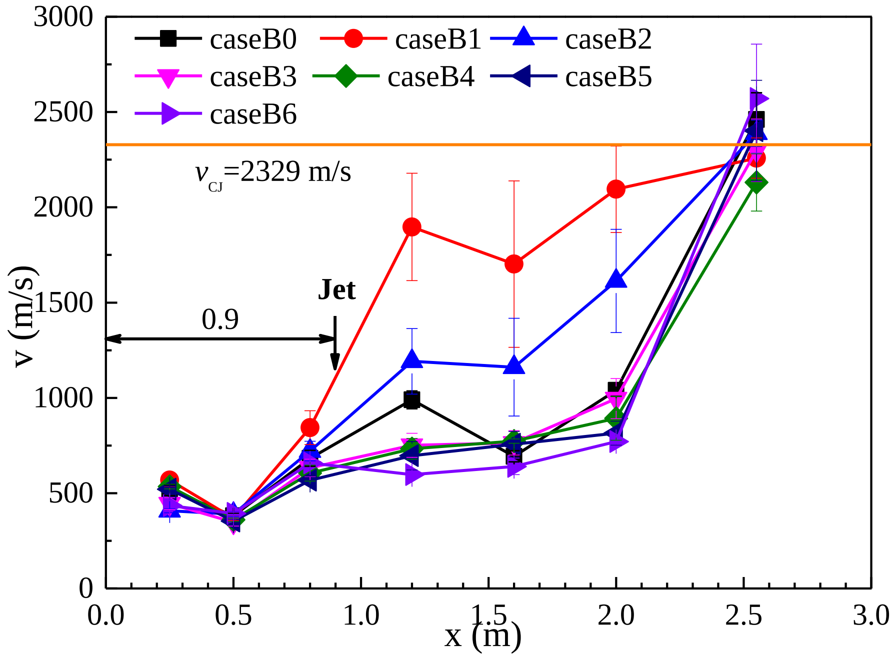

Fig. 5 Velocity of the lead wave with different time duration of argon jet injection, t_i.

Figure 5 shows the wave propagation velocity for different cases. Compared with the baseline case B0, the case with an injection t_i = 25 ms (Case B2) still shows a noticeable wave acceleration in the fast deflagration regime. However, increasing further the injection time (case B3), the velocity behavior approaches to the baseline trend without demonstrating anymore acceleration effect. For cases B4 to B6, the argon jet appears to have an adverse effect weakening the wave propagation. Hence, argon injection with a short injection duration (e.g., t_i = 15 ms, case B1) has an enhancement effect on the wave propagation. On the contrary, by introducing high pressure argon jet with long injection time, the local argon concentration therewith increases and as a result, prohibiting the flame acceleration.

3.3 The effect of turbulence intensity

The experimental conditions in Table 3 are designed to examine the turbulence intensity effect. P_i and t_i are set as variables to ensure the volume of argon injected into the tube remains the same. To minimize the influence of local concentration, the amount of argon injected into the tube is maintained with a small value in these experiments.

Table 3 Injection parameters for experiments with varying turbulence intensities.

Case #	P_i/kPa	t_i/ms	Position
C0	0	0	N/A
C1	100	50	A
C2	150	21	A
C3	200	15	A

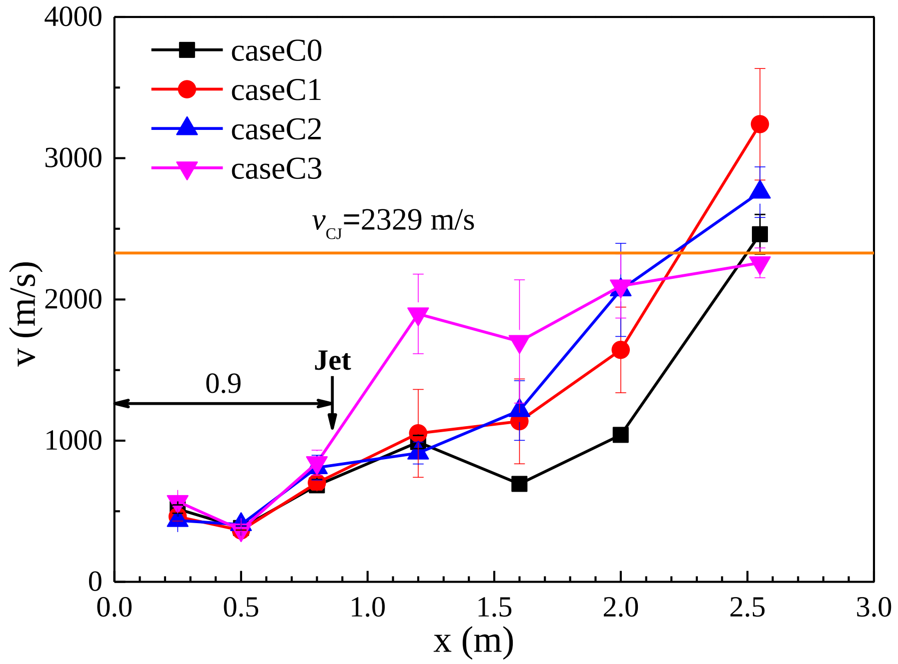

Fig. 6 Velocity of the leading wave with different P_i and t_i for varying turbulence intensity.

Figure 6 shows the wave propagation velocity with different turbulence intensities. The jet location is also highlighted. The propagation velocities of cases C1 to C3 accelerate apparently by comparing with the baseline case C0. In the slow deflagration region where the flow does not experience turbulence generated by the jet, the propagation velocities of all four cases are very close, again about ~500 m/s. After the injection at position A, x = 0.8 m, the velocity for case C3 accelerates rapidly, and this acceleration performance is better than cases C1 and C2. Wave acceleration can only be seen from SP6 (x = 1.6 m) for cases C1 and C2, reaching a velocity of 1570 m/s and 2045 m/s, respectively, at the position of SP7. By comparing with the baseline case, the results demonstrate again that higher turbulence intensity enhances the acceleration of the flame propagation. Therefore, when the concentration of the argon gas is at a low level, the turbulence dominates the wave propagation and DDT process.

3.4 The effect of injection position

Three jet positions are chosen to examine the injection position effect on DDT and wave propagation behavior. The distance between position C and SP1 is 10 cm (here 0 in the x-axis represents the first shock pin location, hence x = - 0.1 m for position C). The other details regarding the jet positions are shown in Fig. 2. The jet parameters of this group are shown in Table 4.

Table 4 Injection parameters for experiments with varying injection location.

Case #	P_i/kPa	t_i/ms	Position	x/m
D0	0	0	N/A	N/A
D1	200	15	A	0.9
D2	200	15	B	1.3
D3	200	15	C	-0.1

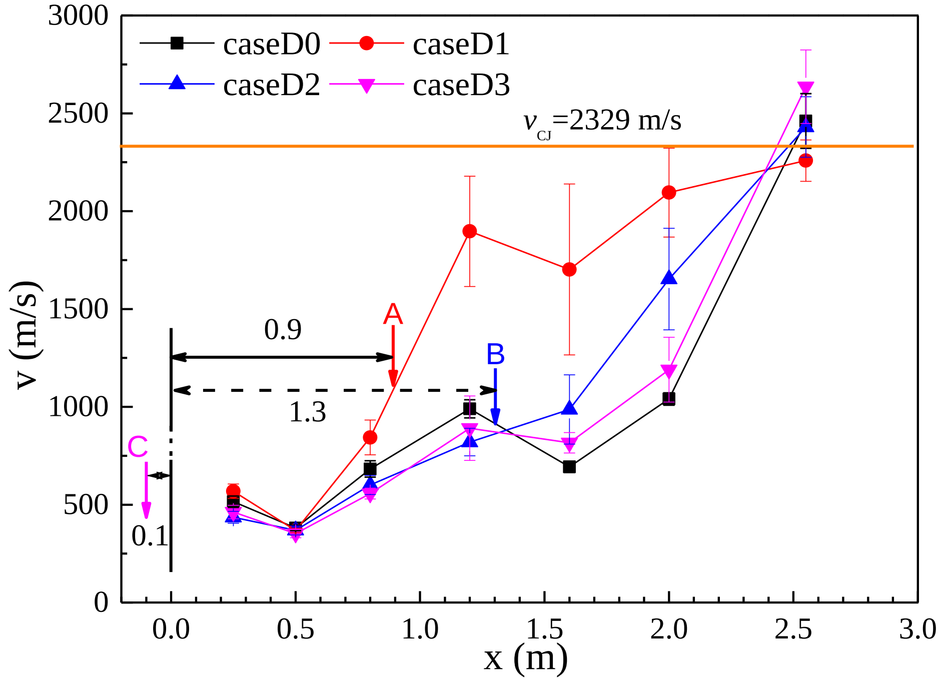

Fig. 7 Velocity of the leading wave with different injection location.

Figure 7 shows the wave velocity behavior during DDT with the argon jet placed at different positions. For the case D1, an enhanced acceleration of the propagation velocity is clearly observed. For the injection position located at the middle of the tube (case D2), only a small enhancement is seen on the wave acceleration. At this position B, the baseline case already shows the wave propagating at a high velocity about 700 m/s supported possibly by a high level of turbulence originated from the evolving flame acceleration process. The added turbulence by the argon jet thus has less prominent effect on such wave condition. For the last case D3 where the jet in introduced in the slow deflagration stage, there is also no significant influence on the wave propagation.

3.5 Effect of the turbulence evolution on the wave acceleration

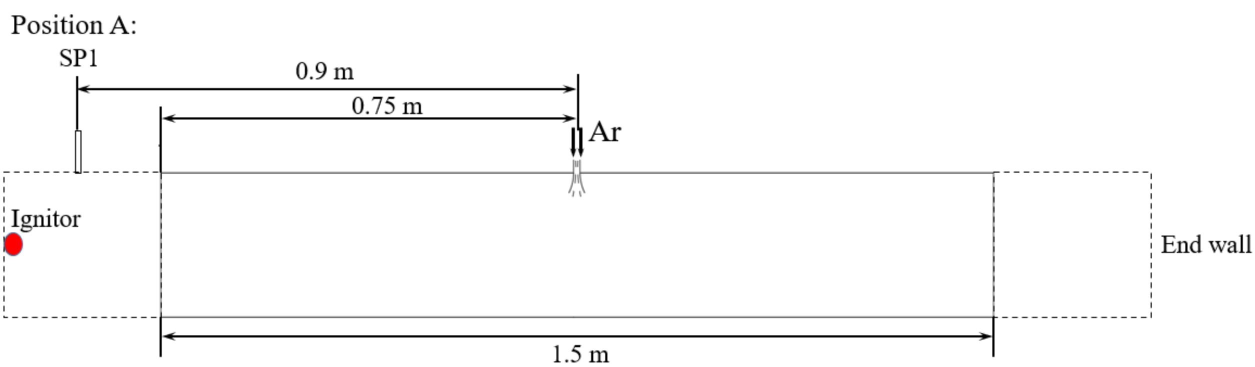

(a)

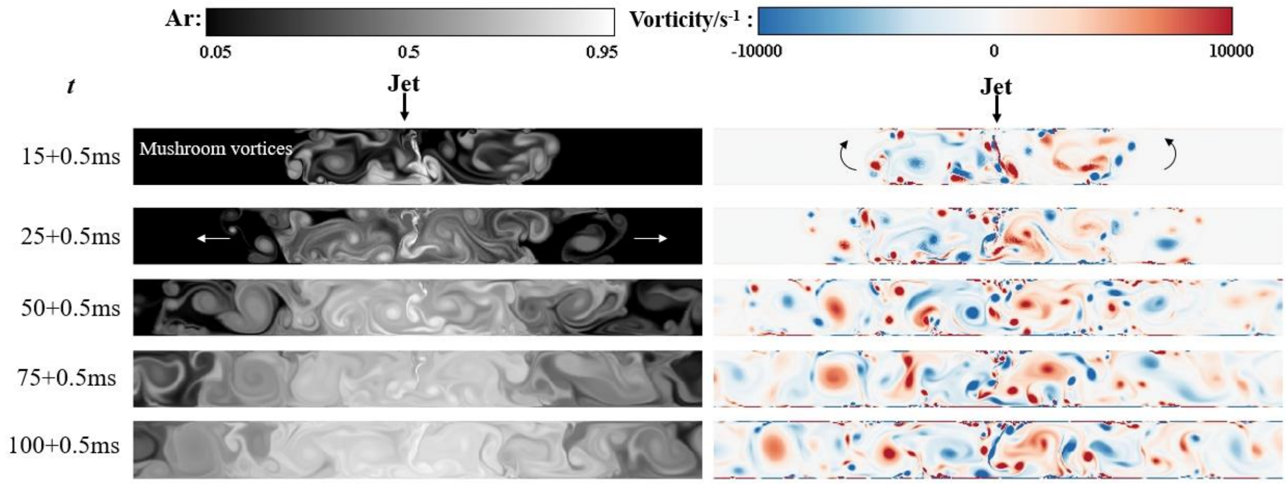

(b)

Fig. 8 The evolution of the distribution of Ar and the vortices formed at position A

The two-dimensional turbulence flow structures generated by argon jet with two different positions are simulated. Fig. 8(b) shows the distribution of Ar and vorticity at corresponding time to the experiments B1~B4 mentioned in Section 3.2 which placed the jet at position A, as shown in Fig. 8(a). It can be seen that the jet has already collided with the bottom wall when t_i is 15 ms, forming mushroom vortices. The vortices formed on the both sides of the jet inversely roll up. The vortices formed earlier are pushed away by the following jet due to the increasing mass of Ar. It is obvious that peripheral vortices gradually dissipate during their paths to the upstream/downstream of the jet, which is due to the collisions from vortex-to-vortex and vortex-to-wall. Note that both the mass of Ar and the vorticity increase with the extending of t_i, hereby a criterion is proposed to evaluate the dominant factor of the concentration and the turbulence on the propagation of flame.

As Ar was considered as an inert gas suppressing the combustion, while the turbulence structure especially the vortices have a positive influence on flame propagation, both the concentration of Ar and the vorticity have been nondimensionalized. The concentration Ar is nondimensionalized with the initial density of mixture:

$$C_{Ar} = \int_A \frac{\rho Y_{Ar}}{\rho_0} dA \tag{1}$$

Where ρ, ρ_0 represent the current mixture density and the initial mixture density respectively; Y_{Ar} is the current mass fraction of Ar; A is the area of the computation domain. The dimensionless treatment of vorticity (*Vor*) can be described as follows:

$$Vor = \int_A \left| \frac{\partial\left(v / v_j\right)}{\partial(x / l)} - \frac{\partial(u / v_j)}{\partial(y / h)} \right| dA \tag{2}$$

Where u, v and v_j are the x velocity component, y velocity component and jet velocity, respectively; l represents the length of the domain, the h represents the height; A is the same as the Equation 1. Thus, a dimensionless criterion factor can be obtained by calculating the ratio between two factors, i.e., Tur_c:

$$Tur_c = \frac{Vor}{C_{Ar}} \tag{3}$$

Fig. 9 shows Tur_c evolves with the jet duration time. Apparently, the curve drops dramatically while jet extending from 15 ms to 50 ms, and it keeps at a relatively stable value from 75 ms to 100 ms. This is in good agreement with the results observed from experiments B1~B4. The results confirm that the positive effect of the turbulence is offset with the development of time, and even be oppressed by the combustion inhibition effect due to the increasing mass of Ar, as the jet duration time is consistently extended.

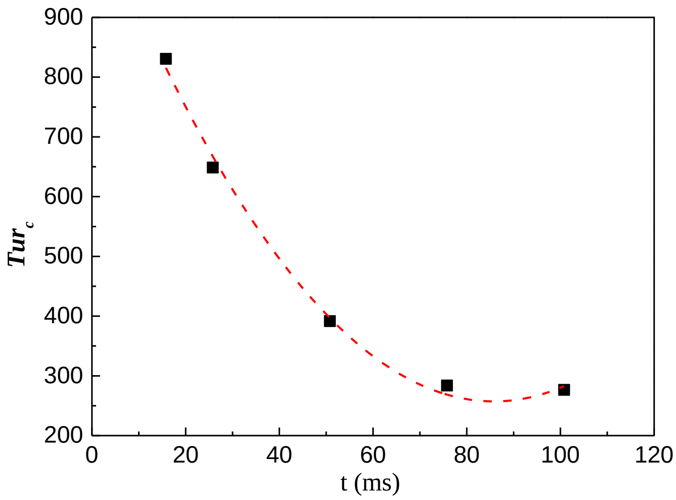

Fig. 9 The tendency of *Vor/C* varied with jet duration time

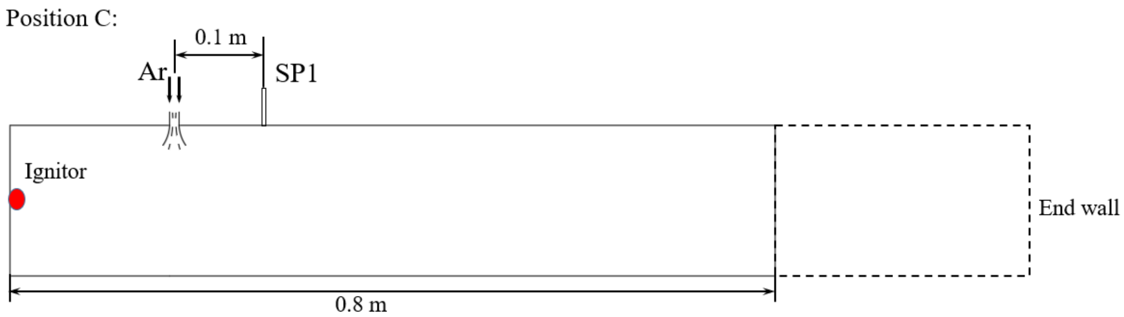

(a)

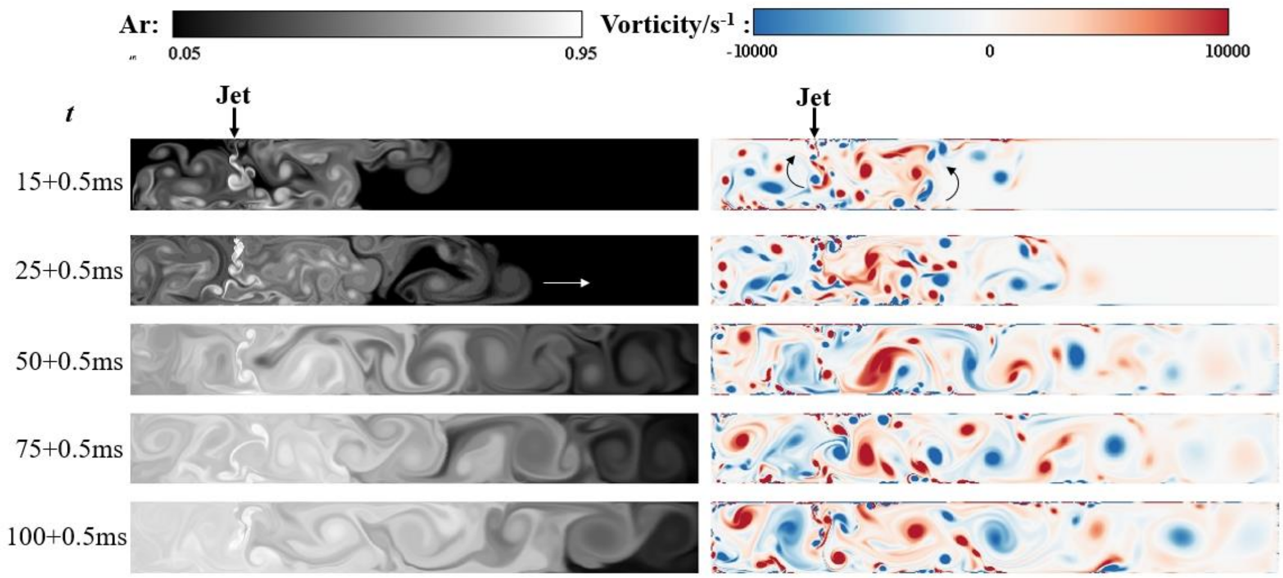

(b)

Fig. 10 The evolution of the distribution of Ar and the vortices formed with jet placed at position C

Fig. 10(b) depicts the Ar distribution and the vortices evolution for the case that with the jet placed at position C (as shown in Fig. 10(a)). The Ar concentration and vortices evolution processes are similar to the case in which the jet placed at position A. The difference between those two positions is that the Ar concentration in position C increases to approximately 1 in the region on the left side of the jet as the jet is placed to the location adjacent to the ignition end wall. This scenario occurred mainly because of the expansion of Ar concentration is constrained by the left wall. However, the Ar injection has a positive effect on the formation of the vortices near the left end wall (clearly shown by the right column of Fig.10(b)). The vortices propagate to the downstream and gradually dissipate, which are similar as the case shown in Fig.8. To verify the competition effect between the negative influence of Ar dilution and the positive influence of the turbulence enhancing the vortices, the dimensionless criterion Tur_c is then calculated and shown in Fig. 11. It can be seen from Fig. 11 that, with the increasing of injection time t_i, the tendency of Tur_c curve presents a monotonous decrease, indicating the dominant factor affecting the DDT behavior is the Ar concentration, rather than the stretch effect of the vortices. It is noteworthy that Ar jet is placed at position C near the ignitor, and therefore the increased Ar concentration with longer t_i greatly inhibits the ignition progress, resulting in a slower flame propagation velocity than the one with the jet placed at position A.

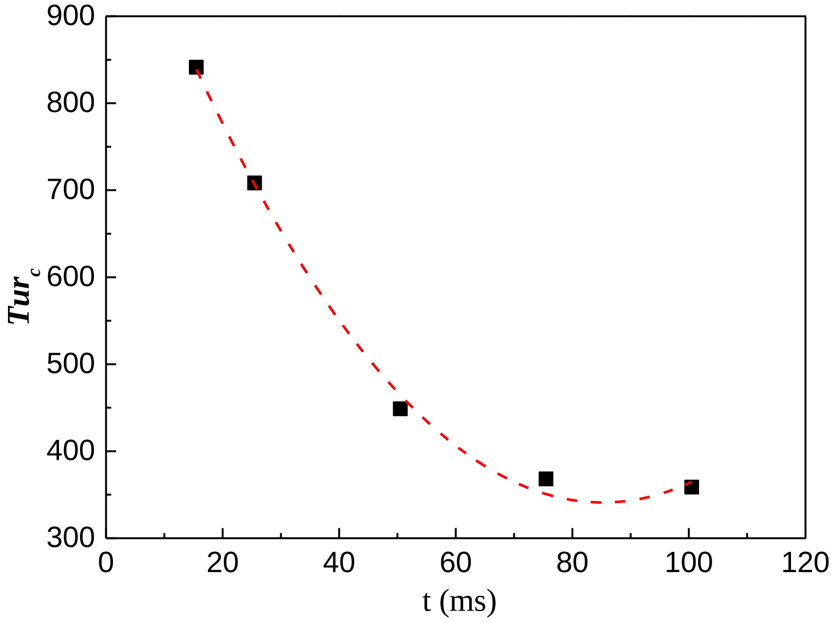

Fig. 11 The tendency of *Vor/C* varied with jet duration time for the jet placed at position C

By comparing the Ar distribution and vortices evolution of the cases with different jet positions, it is obvious that as a jet having a shorter distance to the ignitor, resulting more Ar concentrate on the left side of the jet contacting the flame front primarily. The suppression effect from the increasing inert gas mass is more prominent than the flame-acceleration effect from vortices. The dimensionless criterion Tur_c is verified to be an adequate parameter to estimate the dominate mechanism in flame propagation and the initial stage of DDT as inert jet is applied for detonation enhancement.

4. Conclusion

With the increasing interest in employing detonation as fast combustion mode for advanced propulsion systems, controlled initiation and rapid onset of detonation from DDT become desirable. In this study, we explore the use of an inert argon jet as an enhancement method by its turbulence generation to promote further flame acceleration and strengthen the lead shock wave for DDT. A series of experiments and numerical simulations were conducted to investigate effects of various injection parameters on DDT, including the initial injection pressure, duration time and jet position. The results show that turbulence generated by argon injection accelerates the wave propagation velocity when the wave is at the fast deflagration regime with velocity above 500 m/s. At such condition, the enhanced DDT process by the jet has no noticeable variation with increasing P_i. However, either a long injection time or an exceeding injection pressure will increase the local argon concentration, and prohibit the wave acceleration. The present study has proved that higher turbulence intensity induced by higher P_i and shorter t_i has better performance on enhancing the DDT. In the experiments, different injection positions also are tested and found have impacted the DDT process. Only an appropriate injection position can make a positive effect on the DDT process. Additionally, by analyzing the experiments and numerical simulations of the cases with different jet positions, the dimensionless criterion Tur_c proposed has demonstrated the dominant factor of the flame propagation. The results show that the suppression effect by Ar dilution is more prominent than the stretch dynamics on the flame acceleration by vortices with the increasing of t_i.

Acknowledgment

This work is supported by the National Natural Science Foundation of China – China (Grant Nos.: 91741114 and11772199).

References:

[1] Roy G D, Frolov S M, Borisov A A, Netzer D W, Pulse detonation propulsion: challenges, current status, and future perspective. Prog Energ Combust 2004;30 (6): 545-672.

[2] Kailasanath K, Recent developments in the research on pulse detonation engines. AIAA Jounral 2003;41 (2): 145-59.

[3] Xiang G, Li H, Cao R, Chen X, Study of the features of oblique detonation induced by a finite wedge in hydrogen-air mixtures with varying equivalence ratios. Fuel 2020;264: 116854.

[4] Xiang G X, Gao X, Tang W J, Numerical study on transition structures of oblique detonations with expansion wave from fnite-length cowl. Phys Fluids 2020;29 (5): 56108.

[5] Zhou R, Wang J P, Numerical investigation of flow particle paths and thermodynamic performance of continuously rotating detonation engines. Combust Flame 2012;159 (12): 3632-45.

[6] Wolański P, Detonative propulsion. Proc Combust Inst 2013;34 (1): 125-58.

[7] Zhang B, Liu H, Yan B J, Velocity behavior downstream of perforated plates with large blockage ratio for unstable and stable detonations. Aerosp Sci Technol 2019;86: 236-43.

[8] Zhang B, Liu H, Wang C, Yan B J, An experimental study on the detonability of gaseous hydrocarbon fuel ‑ oxygen mixtures in narrow channels. Aerosp Sci Technol 2017;69: 193-200.

[9] Zhang B, Liu H, Theoretical prediction model and experimental investigation of detonation limits in combustible gaseous mixtures. Fuel 2019;258: 116132.

[10] Zhang B, Liu H, Yan B, Ng H D, Experimental study of detonation limits in methane-oxygen mixtures: Determining tube scale and initial pressure effects. Fuel 2020;259: 116220.

[11] Zhang B, Detonation limits in methane-hydrogen-oxygen mixtures: Dominant effect of induction length. Int J Hydrogen Energ 2019;44 (41): 23532-7.

[12] Zhang B, Liu H, Wang C, On the detonation propagation behavior in hydrogen-oxygen mixture under the effect of spiral obstacles. Int J Hydrogen Energ 2017;42: 21392-402.

[13] Cao W, Gao D, Ng H D, Lee J H S, Experimental investigation of near-limit gaseous detonations in small diameter spiral tubing. Proc Combust Inst 2019;37 (3): 3555-63.

[14] Gao Y, Ng H, Lee J H S, Near-limit propagation of gaseous detonations in thin annular channels. Shock Waves 2017;27 (2): 199-207.

[15] Gao Y, Zhang B, Ng H D, Lee J H S, An experimental investigation of detonation limits in hydrogen-oxygen-argon mixtures. Int J Hydrogen Energ 2016;41: 6076-83.

[16] Gao Y, Lee J H S, Ng H D, Velocity fluctuations near the detonation limits. Combust Flame 2014;161 (11): 2982-90.

[17] Lee J H S, The detonation phenomenon, Cambridge University Press, 2008.

[18] Zhang B, Mehrjoo N, Ng H D, Lee J H S, Bai C H, On the dynamic detonation parameters in acetylene-oxygen mixtures with varying amount of argon dilution. Combust Flame 2014;161 (5): 1390-7.

[19] Zhang B, Kamenskihs V, Ng H D, Lee J H S, Direct blast initiation of spherical gaseous detonations in highly argon diluted mixtures. Proc Combust Inst 2011;33 (2): 2265-71.

[20] Zhang B, Ng H D, Lee J H S, Measurement and relationship between critical tube diameter and critical energy for direct blast initiation of gaseous detonations. J Loss Prevent Proc 2013;26: 1293-9.

[21] Zhang B, Ng H D, Lee J H S, Measurement and scaling analysis of critical energy for direct initiation of gaseous detonations. Shock Waves 2012;22: 275-9.

[22] Bai C H, Zhang B, Xiu G L, Liu Q M, Chen M, Deflagration to detonation transition and detonation structure in diethyl ether mist/aluminum dust /air mixtures. Fuel 2013;107: 400-8.

[23] Wang C, Zhao Y Y, Zhang B, Numerical simulation of flame acceleration and deflagration-to-detonation transition of ethylene in channels. J Loss Prevent Proc 2016;43: 120-6.

[24] Wu M, Kuo W, Accelerative expansion and DDT of stoichiometric ethylene/oxygen flame rings in micro-gaps. Proc Combust Inst 2013;34 (2): 2017-24.

[25] Zhang B, Liu H, The effects of large scale perturbation-generating obstacles on the propagation of detonation filled with methane-oxygen mixture. Combust Flame 2017;182: 279-87.

[26] Zhang B, The influence of wall roughness on detonation limits in hydrogen-oxygen mixture. Combust Flame 2016;169: 333-9.

[27] Shchelkin K I, Influence of tube roughness on the formation and detonation propagation in gas. J Exp Theor Phys 1940;(10): 823-7.

[28] Ciccarelli G, Dorofeev S, Flame acceleration and transition to detonation in ducts. Prog Energ Combust 2008;34 (4): 499-550.

[29] Dorofeev S B, Flame acceleration and explosion safety applications. Proc Combust Inst 2011;33 (2): 2161-75.

[30] Goodwin G B, Houim R W, Oran E S, Shock transition to detonation in channels with obstacles. Proc Combust Inst 2017;36 (2): 2717-24.

[31] Cooper M, Jackson S, Austin J, Wintenberger E, Shepherd J E, Direct Experimental Impulse Measurements for Detonations and Deflagrations. J Propul Power 2001;18 (5): 1033-41.

[32] Knox B W, Forliti D J, Stevens C A, Hoke J L, Schauer F R, A comparison of fluidic and physical obstacles for deflagration-to-detonation transition, 49th AIAA Aerospace Sciences

Meeting including the New Horizons Forum and Aerospace Exposition, Orlando, Florida, 2011.

[33] Chambers J M, Ahmed K A, Investigation of Flame Regimes for Flame Acceleration to Detonation, 2018 Joint Propulsion Conference, Cincinnati, Ohio, 2018.

[34] McGarry J P, Ahmed K A, Flame-turbulence interaction of laminar premixed deflagrated flames. Combust Flame 2017;176: 439-50.

[35] McGarry J P, Ahmed K A, Laminar Deflagrated Flame Interaction with a Fluidic Jet Flow for Deflagration-to-Detonation Flame Acceleration, 51st AIAA/SAE/ASEE Joint Propulsion Conference, Orlando, FL, 2015.

[36] Chambers J, Ahmed K, Turbulent flame augmentation using a fluidic jet for Deflagration-to-Detonation. Fuel 2017;199: 616-26.

[37] Tarrant D J, Chambers J M, Ahmed K A, Fast flame interaction with high pressure turbulent jets for turbulent deflagration-to-detonation transition, 2018 Joint Propulsion Conference, Cincinnati, Ohio, 2018. DOI: 10.2514/6.2018-4780

[38] Peng H, Huang Y, Deiterding R, Luan Z, Xing F, You Y, Effects of jet in crossflow on flame acceleration and deflagration to detonation transition in methane-oxygen mixture. Combust Flame 2018;198: 69-80.

[39] Zhang B, Chang X Y, Bai C H, End-wall ignition of methane-air mixtures under the effects of CO2/Ar/N2 fluidic jets. Fuel 2020;270: 117485.

[40] Bai C H, Chang X Y, Zhang B, Impacts of turbulence on explosion characteristics of methane-air mixtures with different fuel concentration. Fuel 2020;271: 117610.

[41] Chang X Y, Zhang B, Ng H D, Bai C H, The effects of pre-ignition turbulence by gas jets on the explosion behavior of methane-oxygen mixtures. Fuel 2020;277: 118190.

[42] Cheng J, Zhang B, Liu H, Wang F, The precursor shock wave and flame propagation enhancement by CO2 injection in a methane-oxygen mixture. Fuel 2021;283: 118917.

[43] Cheng J, Zhang B, Liu H, Wang F, Experimental study on the effects of different fluidic jets on the acceleration of deflagration prior its transition to detonation. Aerosp Sci Technol 2020: In Press.

[44] Ding J, Liang Y, Chen M, Zhai Z, Si T, Luo X, nteraction of planar shock wave with three-dimensional heavy cylindrical bubble. Phys Fluids 2018;30: 106109.

Effects of inert gas jet on the transition from deflagration to detonation in a stoichiometric methane-oxygen mixture

Jun Cheng[1], Bo Zhang[1†], Hoi Dick Ng[2], Hong Liu[1], Fuxing Wang[1]

[1]Shanghai Jiao Tong University
School of Aeronautics and Astronautics, Shanghai, 200240, China

[2] Concordia University
Department of Mechanical, Industrial and Aerospace Engineering
Montréal, QC, H3G 1M8, Canada

Declaration of interests

☒ The authors declare that they have no known competing financial interests or personal relationships that could have appeared to influence the work reported in this paper.

☐The authors declare the following financial interests/personal relationships which may be considered as potential competing interests:

CRediT authorship contribution statement

Jun Cheng: Investigation, Data collection & analysis , Methodology.

Bo Zhang: Investigation, Validation, Writing - review & editing

Hong Liu: Supervision

Fuxing Wang: Supervision